LARGE-SCALE NUMERICAL AERODYNAMIC SIMULATIONS FOR COMPLETE AIRCRAFT CONFIGURATIONS

Susumu Takanashi

National Aerospace Laboratory
7-44-1 Jindaiji-Higashi, Chofu, Tokyo
182 Japan

ABSTRACT

Navier-Stokes simulations of transonic flows are carried out for complete configurations of two kinds of test models which were designed to investigate the aerodynamic characteristics of the developing airplanes using the transonic wind tunnel.

An O-O grid system for the computation is constructed by the automatic procedure based on the electro-static theory. The Reynolds-averaged Navier-Stokes equations are solved on a supercomputer, FACOM VP-400,using an implicit finite volume, upwind TVD scheme.

Computed pressure distributions as well as force coefficients are also compared with the experimental data.

1. Introduction

In recent years, great progress has been made in the development of numerical methods of computing potential, Euler, and Navier-Stokes equations for complex three-dimensional flows. The existing computer codes based on the Navier-Stokes equations, however, require not only large CPU time, but also laborious, time-consuming grid generation procedure, as far as complex configuration concerned. In order to make computer codes useful, just as wind tunnel itself, substantial improvements have to be made.

In view of this situation , a numerical wind tunnel was newly developed at the National Aerospace Laboratory in order to efficiently obtain the numerical aerodynamic design data for practical aircraft configurations in the development stage. The numerical wind tunnel consists of a number of computer programs which are running on a Japanese supercomputer, FACOM VP-400, having ability of one giga FLOPS and one giga BYTE memory.

Most important parts of the programs are the Navier-Stokes solver and the grid generator. The Reynolds-averaged thin-layer Navier-Stokes equations are numerically solved by a TVD upwind scheme [1] which is presently considered as one of the most reliable and accurate schemes, especially for the flow with strong shock waves. A new method of automatic grid generation for block-structured grids is developed, which is based on the elector-static theory.

Major objectives of this paper are (1) to describe the automatic grid generation procedure, (2) to present the latest results computed using the newly obtained grids, and (3) to demonstrate the reliability and accuracy of the numerical wind tunnel comparing with the experimental data.

2. Automatic Grid Generation

The advent of high-speed and large memory supercomputers has made it possible to numerically simulate the compressible viscous flows about complex geometries. These numerical solutions are all obtained by firstly-generating high-quality grids around the bodies to discretize the Navier-Stokes equations.

In the last decade, a number of different methods of grid generation have been proposed by many researchers [2,3]. Every method, however, seems to have its own strength as well as weakness. Consequently, a CFD researcher has chosen the most appropriate one among them, taking into account the geometrical complexity, computing cost for generation, grid topology, or other factors.

One of the most powerful and promising methods is a boundary element method which is based on Laplace equation. The grid generation procedures belonging to this category have been developed by Sikora et al. [4] and also by the present author[5].

Although both smoothness and orthogonality of such kind of grid are certainly excellent in the whole flowfield, an essential limitation lies on the large computer time required for the calculation of the influence coefficients including several elementary functions such as 'arcsinh'. This approach will become prohibitive as the total number of grid points exceeds a million.

The objective of this section is to propose an alternative approach to the generation of a structured grid without loss of the excellent properties inherent in Laplace equation, and also to show the great reduction of CPU time, by which it became possible to generate a block-structured grid for a nearly-complete aircraft configuration.(Although the almost same grid generation algorithm has been proposed by the present author in Ref.6, more detailed description will be given in this paper.)

To generate an O-O grid inside the region between a body and an arbitrary closed outer boundary, e.g. an infinitely large sphere, we first consider the electro-static field produced by the point charges distributed on the boundaries. Following Coulomb's law, the electric force vector, $\mathbf{F}$, can be expressed as

$$\mathbf{F} = \sum_j \frac{q_j}{r_j^2} \frac{\mathbf{r}_j}{r_j} \qquad (1)$$

where $\mathbf{r}_j$ is the vector drawn from the j-th boundary point to an arbitrary point in space, r_j is the length of the vector, and q_j is the amount of point charge at the j-th point.

The charge q_j can be determined by an appropriate boundary condition. Assuming that the total amount of charges on each boundary is fixed at a specified value, the electro-static vector field is uniquely determined as will be shown later. Therefore we can draw the electric force line starting at each inner boundary point and going toward the outer boundary. Next, placing grid points regularly along the electric force lines, an O-O grid system is obtained in space. The determination of charge distribution can be reduced to a non-linear minimization problem with a linear constraint.

Let $\mathbf{n}_i$ be a specified normal unit vector at the i-th boundary point and be the electric force vector at the point located at a very small distance, in the direction of $\mathbf{n}_i$, from the i-th boundary point. Stipulating that the direction of the vector $\mathbf{F}_i$ coincides with that of $\mathbf{n}_i$, i.e. $\mathbf{n}_i \times \mathbf{F}_i = 0$, the problem is equivalently to minimize the functional G defined by

$$G = \sum_i (| \mathbf{n}_i \times \mathbf{F}_i |)^2 \qquad (2)$$

with the constraint defined by

$$\begin{aligned} &\sum_j q_j = T \quad \text{for inner boundary} \\ \text{and} \quad &\sum_j q_j = -T \quad \text{for outer boundary} \end{aligned} \qquad (3)$$

where T is an arbitrary constant.

Although several techniques have been developed to solve such an optimization problem [7], we adopt here a simple iteration method suitable for a big system of linear equations to determine the charge distribution.

The functional G is a quadratic function of qj, i.e.

$$\begin{aligned} G = {} & c_{11}q_1^2 + c_{12}q_1q_2 + \cdots + c_{1n}q_1q_n \\ & + c_{21}q_2q_1 + c_{22}q_2^2 + \cdots + c_{2n}q_2q_n \\ & \cdots\cdots\cdots\cdots\cdots\cdots \\ & + c_{N1}q_Nq_1 + c_{N2}q_Nq_2 + \cdots + c_{NN}q_N^2 \end{aligned} \qquad (4)$$

where N is the total number of boundary points, and c_{lm} (l,m = 1,...,N) are the coefficients depending only on both the coordinates of the boundary points and the directions of the specified unit vectors.

Since $\frac{\partial G}{\partial q_j} = 0$ (j = 1,...,N) at the minimum of G, the following linear equations are obtained.

$$\begin{aligned} & a_{11}q_1 + a_{12}q_2 + \cdots + a_{1N}q_N = 0 \\ & a_{21}q_1 + a_{22}q_2 + \cdots + a_{2N}q_N = 0 \\ & \cdots\cdots\cdots\cdots\cdots\cdots \\ & a_{N1}q_1 + a_{N2}q_2 + \cdots + a_{NN}q_N = 0 \end{aligned} \qquad (5)$$

where $a_{lm} = c_{lm} + c_{ml}$. This linear system can be solved subject to the constraint using the point relaxation technique.

Firstly assuming that the initial values of q_j to be

$$\begin{aligned} &q_j^{(0)} = 1/N_{inner} \quad \text{for inner boundary} \\ \text{and} \quad &q_j^{(0)} = -1/N_{outer} \quad \text{for outer boundary} \end{aligned}$$

where N_{inner} and N_{outer} are the total numbers of the inner and outer boundary points, respectively, we get the intemediate 'Point Jacobian' solution q'_j

as

$$q'_j = (1-\omega)\, q_j^{(0)} + \omega \left(\frac{-\sum_{m \neq j} a_{jm} q_m^{(0)}}{a_{jj}} \right) \quad (6)$$

where ω is a relaxation parameter which is chosen to be less than unity. These newly obtained values have to be adjusted to satisfy the constraint as well as an additional condition that the charges are positive for the inner boundary and negative for the outer boundary. More precisely, the first approximation of the optimum charge distrubution is written as

$$q_j^{(1)} = \frac{T}{\sum_{\text{inner}} q''_j}\, q''_j \quad \text{for inner boundary} \quad (7)$$

$$\text{with} \quad q''_j = \begin{cases} q'_j & \text{for } q'_j > 0 \\ \varepsilon & \text{for } q'_j \leq 0 \end{cases}$$

and

$$q_j^{(1)} = \frac{-T}{\sum_{\text{outer}} q''_j}\, q''_j \quad \text{for outer boundary} \quad (8)$$

$$\text{with} \quad q''_j = \begin{cases} q'_j & \text{for } q'_j < 0 \\ -\varepsilon & \text{for } q'_j \geq 0 \end{cases}$$

where T=1 and ε is a small positive constant. The same process is iterated until some user-specified convergence criterion is satisfied.

As long as the density of boundary points is sufficiently large, it is expected that the solution is unique and the functional very small, because a set of dense discrete points at each boudary can be regarded as a continuous surface of conductor which yields an unique electro-static vector field for specified amounts of boundary charges.

The computer program for the force vector F includes only one 'SQRT' and also only several statements of simple arithmetic operations. In addition, all the variables relating to the boundaries can be completely vectorized in one dimension. As a result this method is much more efficient than the conventional boudary element methods. In fact it takes only 50 minutes to generate one million grid points in space without any interpolation when a FACOM VP-400 is used.

To illustrate the capability of the present method, two simple examples are given in Figs.1 and 2. Fig.1 shows an O-O grid about an axisymmetric concave-convex mixed body surrounded by a sphere, which satisfies orthogonality condition on both inner and outer boundaries. The grid points along each electric force line are exponetially clustered near the body surface as in the most typical technique for the Navier-Stokes Computation. In Fig.2 is demonstrated the flexibility of the present method : The concentration of grid lines near the concave part of the body can be considerably lessened by imposing, as the new boundary condition, the use of the inclined vector instead of the original normal vector used in the first example. As seen in the second example, the direction of unit vector specified at the boundaries can effectively control the grid lines in space. Special emphasis is put on the fact that the orthogonalization of grid lines near the body surface can be automatically realized even for the non-orthogonality condition imposed, as in the second example, as long as the first grid point is chosen to be on the line normal to the body surface(see Fig.2(d)).

It should be noted that the present method can not generate O-O grid for the singular configuration which is not homeomorphic to a sphere. The body having a hole like the flow-through nacelle is the case. This difficulty, however, can be overcome by making the configuration homeomorphic, i.e. closing the hole with an infinitely thin film. Therefore the present method may be said to be applicable to a wide range of configurations including a complex combination of fuselage, wing, tail, strut, engine-nacelle, pylon, strake, canard, winglet, and other elements.

3. Navier-Stokes Computation

The first application of the O-O grid generated by the present method has been made to Navier-Stokes simulation for a Mini-Shuttle 'HOPE' configuration which is under development at the National Space Development Agency of Japan [8].The surface grid of HOPE consists of six blocks, each of which has a different number of surface grid points (I,J) as shown in detail in Figs.3(a) and 3(b). Correspondingly the flowfield itself is also divided into six blocks (Figs.3(c) and 3(d)). The total number of space grid points (I,J,K) in one half of the whole space is approximately 0.9 million.All the grid points at the block interfaces are set to be common with each other. As a result the Navier-Stokes computation proceeds without any unfavorable numerical instability,

because an excess interpolation of physical quantities can be avoided with this grid system.

The flow simulation for HOPE was carried out using the Navier-Stokes solver developed by M. Tachibana [9], which employs an implicit finite volume method based on a TVD upwind scheme similar to that of Chacravathy [1]. Baldwin-Lomax turbulence model is used in this computation . In spite of the use of a block-structured grid, computational efficiency is comparable to that for a single-block topology. This encouraging result greatly owes to the fact that the vector variables in the computer program have, as a whole, long lengths of data. The computation time required on a FACOM VP-400 is approximately 12 hours for the 0.9 million grid points used in the symmetrical flow computation for HOPE. Fig.4 shows the surface pressure contours at a Mach number of 0.9 , an angle of attack of 5 °,a yaw angle of 0 °, and a Reynolds number of 10^7 .

The comparisons of the computed force coefficients with the experimental data obtained from the Transonic Wind Tunnel of National Aerospace Laboratory are shown in Fig.5. Except for the drag coefficients the agreement is excellent even for the side force coefficient in the a-symmetrical flow at a yaw angle of 5 °. The discrepancy in the drag has twofold reasons. One is the large aerodynamic interaction due to the existence of the sting behind the base of the model used in the wind tunnel test. The other is the turbulence modeling of the base flow in the computation.

The second example is for a transonic aircraft configuration developed by the Japan Aircraft Developmant Cooperation. Figs.6(f) and 6(b) show the surface grid which consists of six blocks as in the previous case. In Figs.6(c) to 6(f) various views of the space grid are depicted. It should be noted that we used 86 points in the normal direction enough to resolve the boundary shear layers. The total number of grid points is approximately 1.2 million. The flow computation at a Mach number of 0.82, an angle of attack of 2 ° , and Reynolds number of 10^6 could be carried out using the same Navier-Stokes Solver without any modification, since the grid topology itself is the same as that of the first example. Figs.7(a) and 7(b) show the computed pressure contours on the aircraft surface and at the plane of symmetry, respectively. Oil flow pattern is shown in Fig.7(c). Detailed comparison of the computed pressure distributions with experimental data obtained from the Transonic Wind Tunnel of National Aerospace Laboratory is shown in Figs.8(a) to 8(c). As a whole the greement may be said to be good. However, large discrepancies are noticed in the pressure distributions on the horizontal wing. The sting suporting the model at the tail of the fuselage affects flowfield strongly near the horizontal tail. This effect produces a fairly large amount of upwash, which can be virtually canceled by making the twist angle of the horizontal tail minus three degrees in the experiment[10]. However, the cancelation is imperfect as seen in Fig.8(c).

4. Conclusions

(1) Automatic grid generation procedure for complex aircraft configurations was proposed.

(2) The numerical wind tunnel based on the present grid generation can be utilized, as a black box, by the general users unfamiliar to special knowledge of computational fluid dynamics.

(3) Acutual applications to Navier-Stokes simulations were made for two typical configurations, i.e. aerospace plane and transonic aircraft configurations.

(4) Those computed results were also compared with experimental data, which show a good applicability and reliability of the numerical wind tunnel.

5. Acknowledgements

The author would like to thank Mr. M. Tachibana for his permission of the use of the Navier-Stokes solver, and to thank both National Space Development Agency of Japan and Japan Aircraft Development Cooperation for their cooperative suport in the present study. He would also like to thank Ms. T. Munemura, Ms. H. Kamata, and Ms. T. Sugaya for their help in preparing the manuscript of this paper.

References

1. S. R. Chacravathy, 'The Versatility

and Reliability of Euler Solvers Based on High-Accuracy TVD Formulations,' AIAA Paper No.86-0424 (1986).

2. J. F. Thompson, Z. U. A. Warsi and C. W. Mastin, 'Numerical Grid Generation,' North-Holland (1985).

3. S.Sengupta, J.Hauser, P. R. Eiseman, and J. F. Thompson, 'Numerical Grid Generation in Computational Fluid Mechanics '88,' Pineridge Press (1988).

4. J. S. Sikora and L. R. Miranda, 'Boundary Integral Grid Generation,' AIAA Paper 85-4088 (1985).

5. S. Takanashi, 'Grid Generation Procedure Using the Integral Equation Method (I),' National Aerospace Laboratory, TR-1009 (1988).

6. S.Takanashi, 'A simple Algorithm of Structured-Grid Generation and Its Application to Efficient Navier-Stokes Computation,' the Proceedings of the International Symposium on Computational Fluid Dynamics-NAGOYA, Nagoya, Japan (1989).

7. G. N. Vanderplaats, 'Numerical Optimization Techniques for Engineering Design,' McGraw-Hill Book Co. (1983).

8. M.Tachibana, S.Takanashi, and T. Akimoto, 'Navier-Stokes Simulation for a Winged Space Vehicle "HOPE" at Subsonic, Transonic, and Supersonic Regimes,' the Proceedings of the 17th International Symposium on Space Technology and Sciences, Tokyo, Japan (to appear).

9. M. Tachibana and S. Takanashi, 'Numerical Simulation of Flow Fields around an Airplane of Complex Geometry,' National Aerospace Laboratory, SP-10 (1989).

10. T. Kaiden, J. Miyakawa, M. Yanagisawa, and K. Amano, 'Comparison with Computation Using Panel Method and Wind Tunnel Test Around Transonic Complete Aircraft, 'National Aerospace Laboratory, SP-9 (1988).

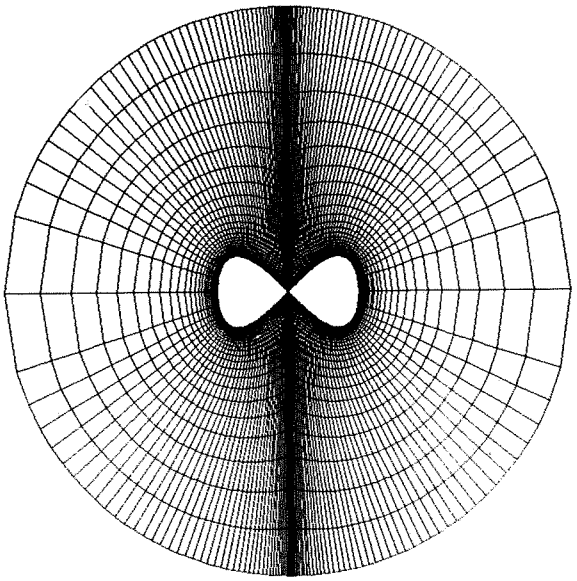

(a) Overall View

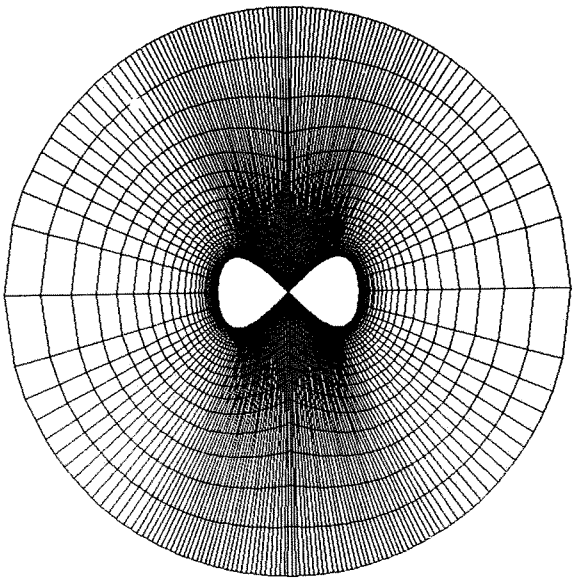

(b) Overall View

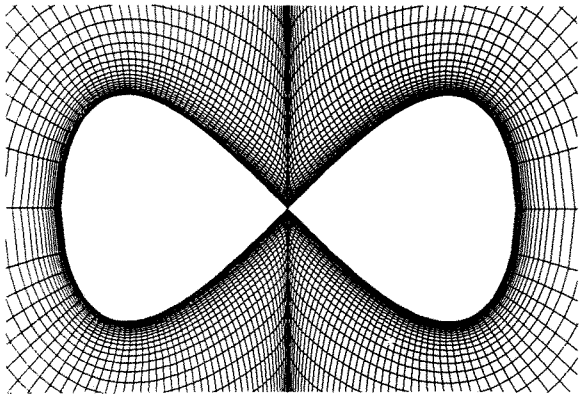

(b) Closeup View

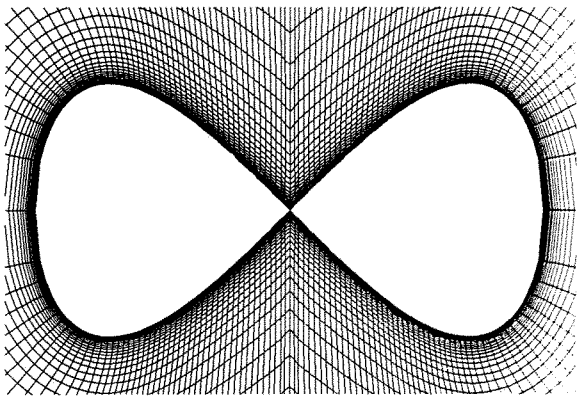

(c) Closeup View

Fig.1 O-O Grid for Axisymmetric Convex-Concave Mixed Body Orthogonality Condition Imposed

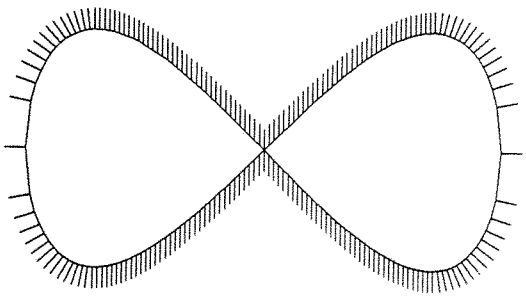

(a) Specified Vectors on Body Surface

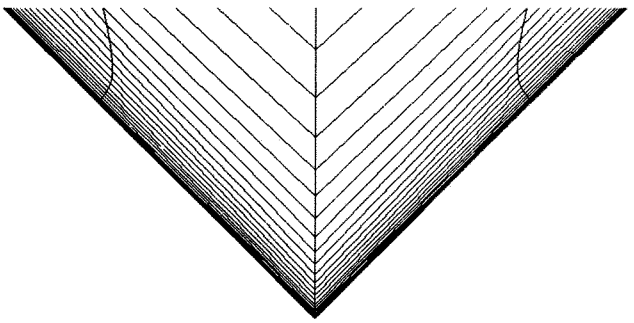

(d) Automatically orthogonalized Grid

Fig.2 O-O Grid for Axisymmetric Convex-Concave Mixed Body Non-Orthogonality Condition Imposed

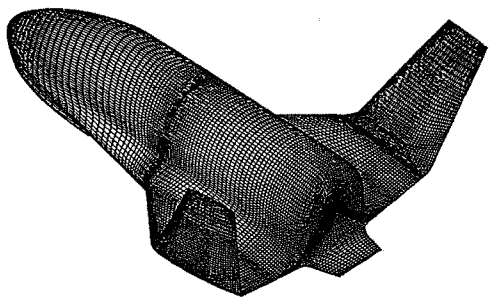

(a) Surface Grid

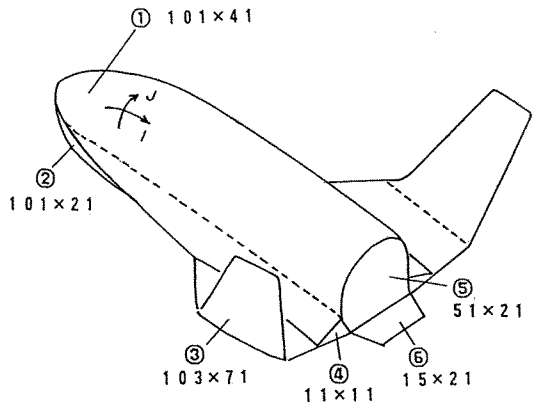

(b) Number of Grid Points at Each Black

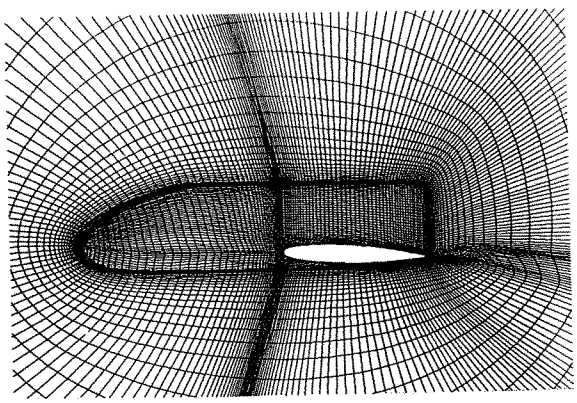

(c) Side View of Grid at Plane of Symmetry

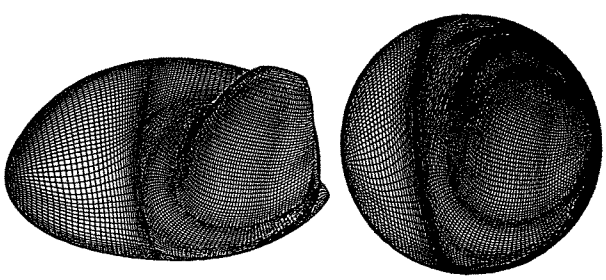

(d) Grid Surface at K=40,60

Fig.3 O-O grid for HOPE Consisting of Fuselage, Strake, Wing, Tip-Fin, and Body-Flap

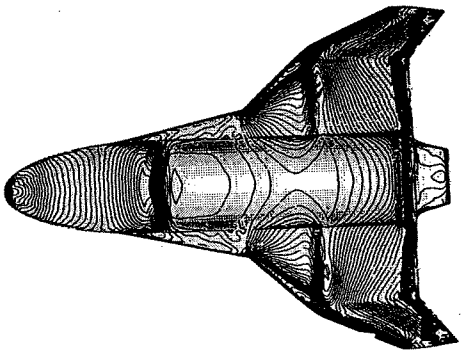

Fig.4 Surface Pressure Contours for HOPE M=0.9 $\alpha=5°$ $R_e=10^7$

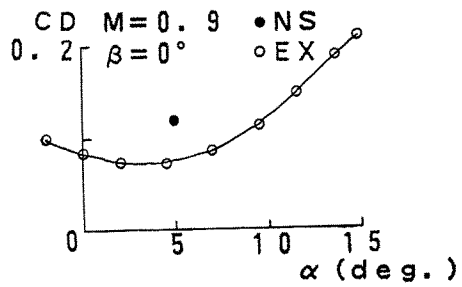

(a) Drag Coefficients

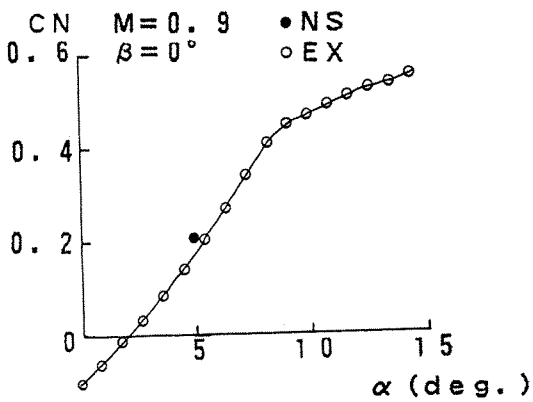

(b) Normal Force Coefficients

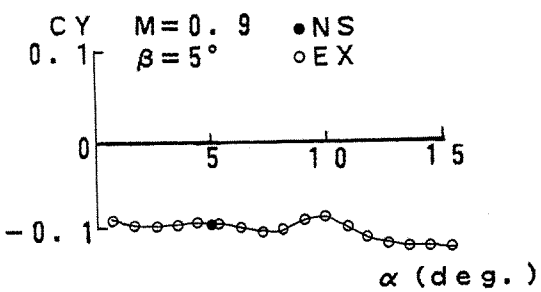

(c) Side Force Coefficients

Fig.5 Comparisons of Computed Force Coefficients with Experimental Data for HOPE M=0.9 $R_e=10^7$

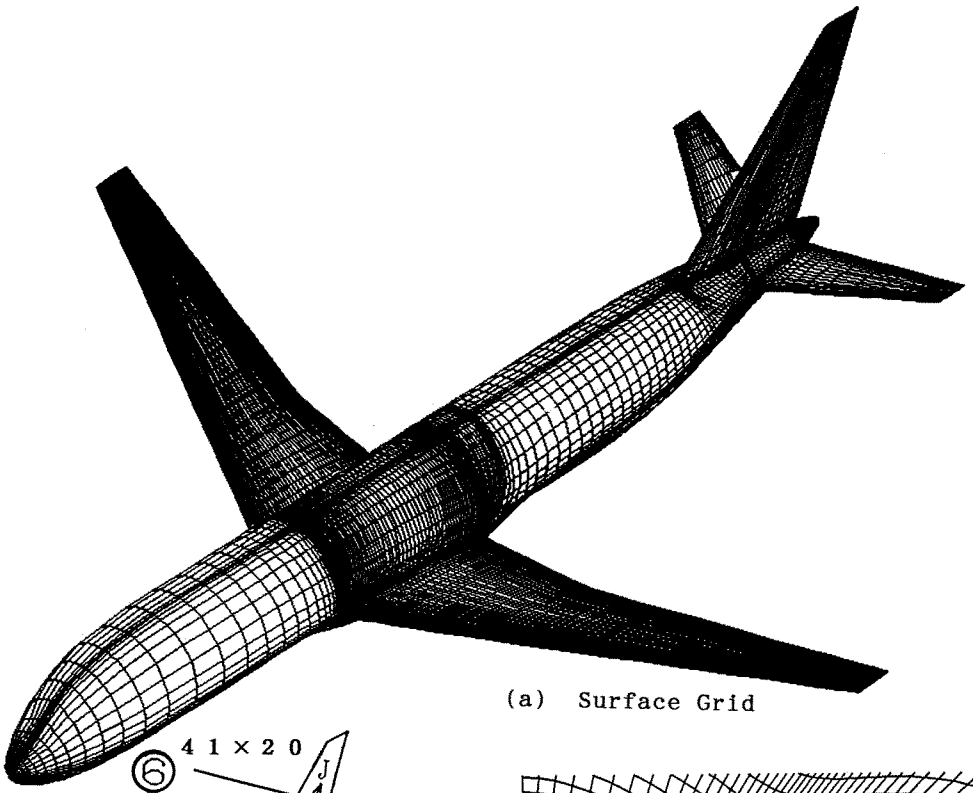

(a) Surface Grid

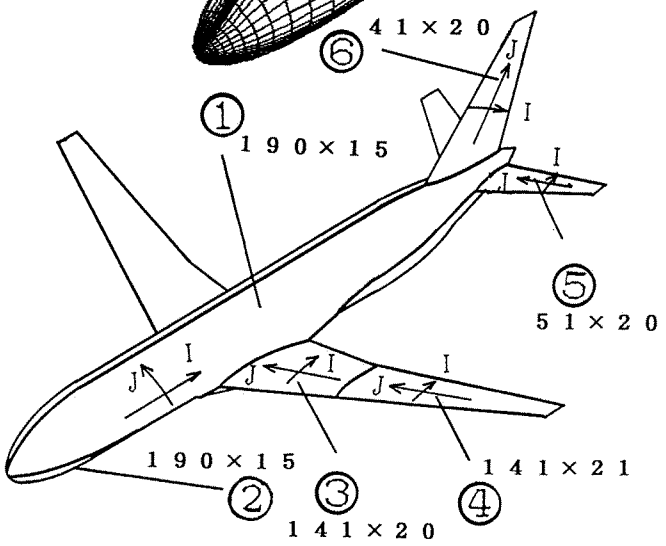

(b) The Number of Surface Grid Points at Each Block

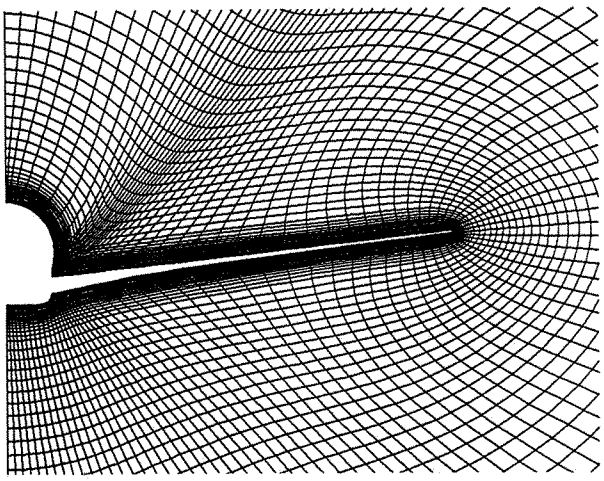

(d) Front View of Grid at Mid-Body Station

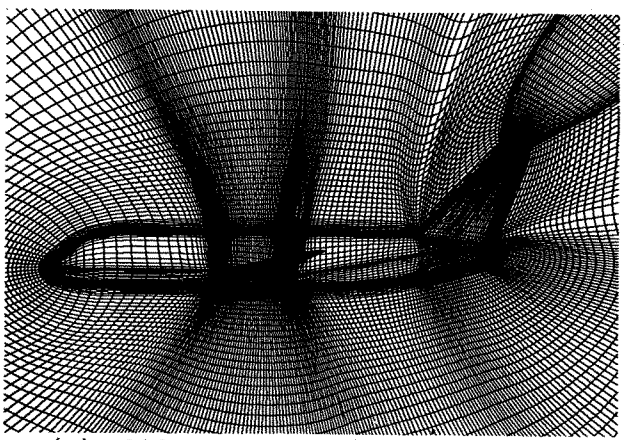

(c) Side View of Grid at Plane of Symmetry

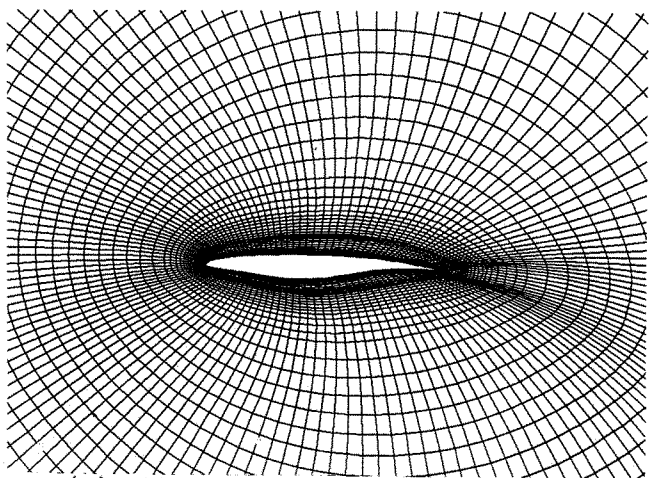

(e) Side View of Grid at Mid-Span Station

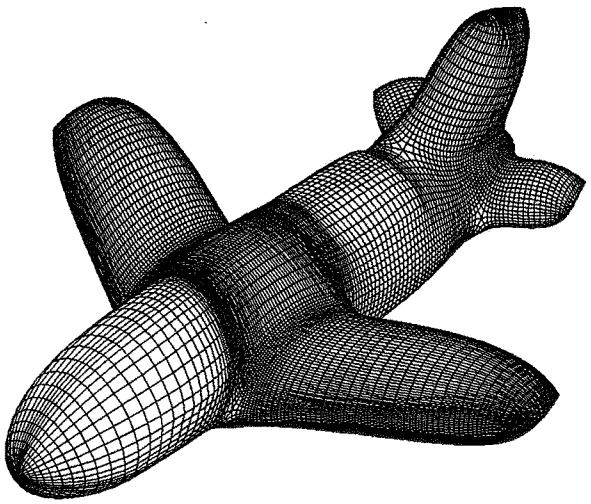

K = 50

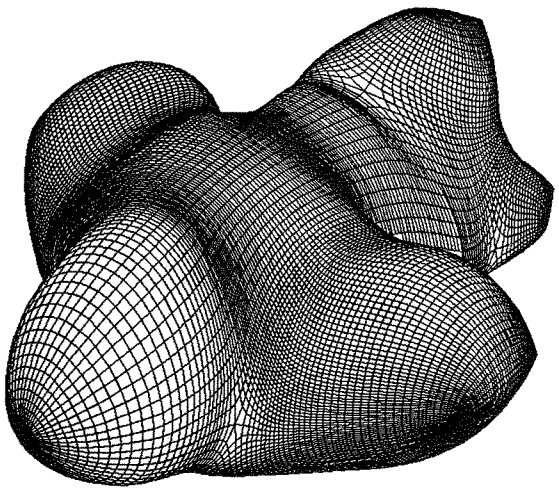

K = 65

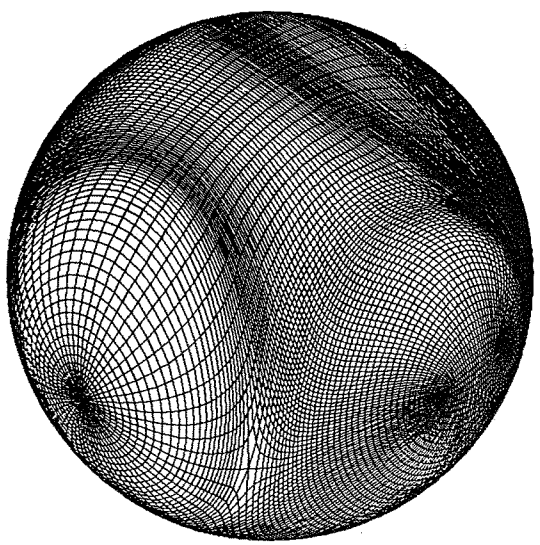

K = 86

(f) Grid Surfaces at K=50,65,86

Fig.6 O-O Grid for Transonic Aircraft Configuration

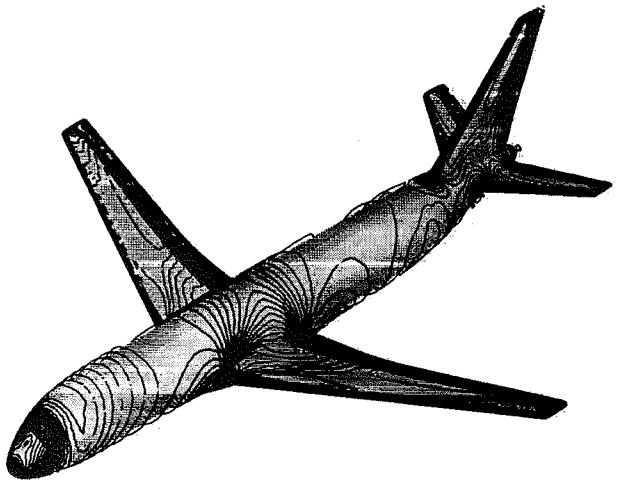

(a) Surface Pressure Contours

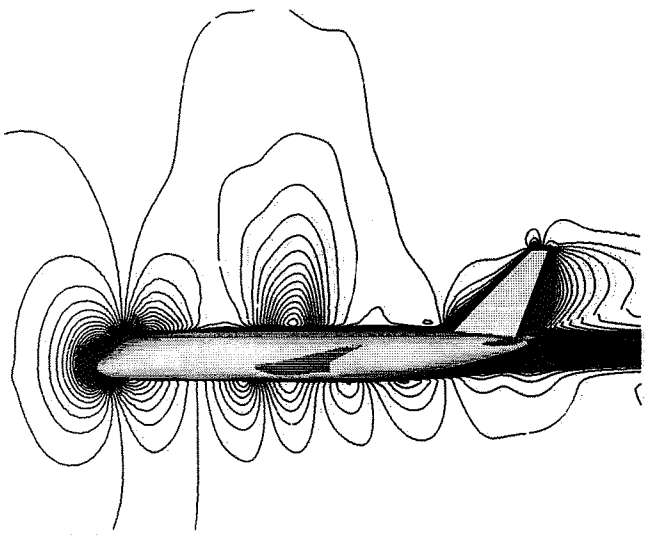

(b) Pressure Contours at Plane of Symmetry

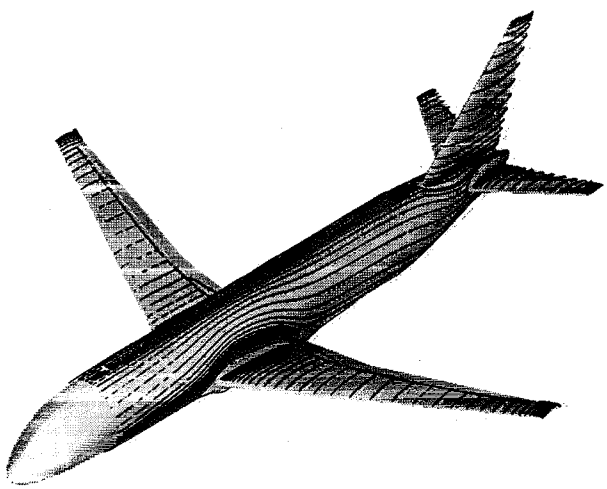

(c) Oil Flow Pattern on Aircraft Surface

Fig.7 Computed Results for Transonic Aircraft Configuration

$M = 0.82 \quad \alpha = 2° \quad R_e = 1.1 \times 10^6$

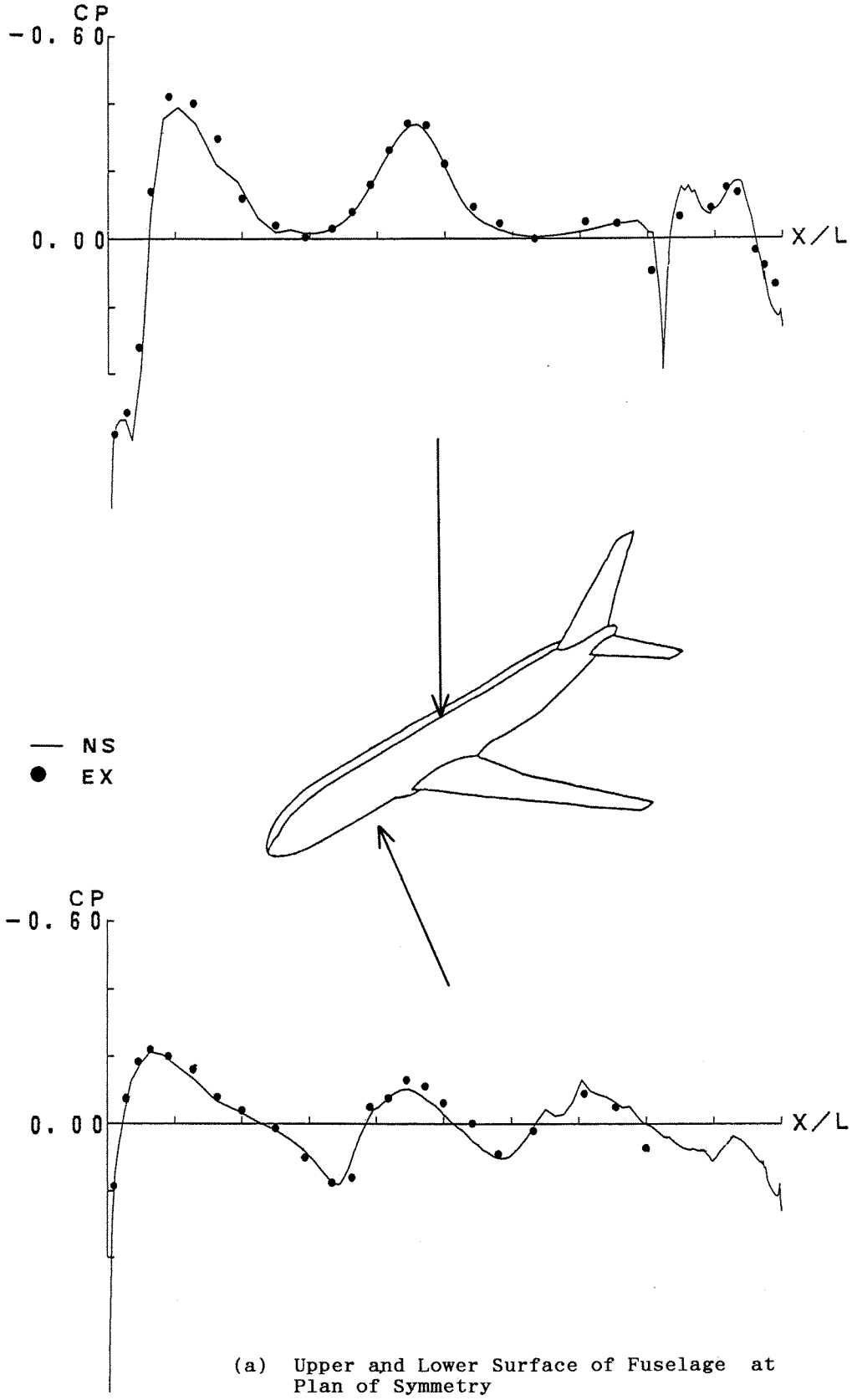

(a) Upper and Lower Surface of Fuselage at Plan of Symmetry

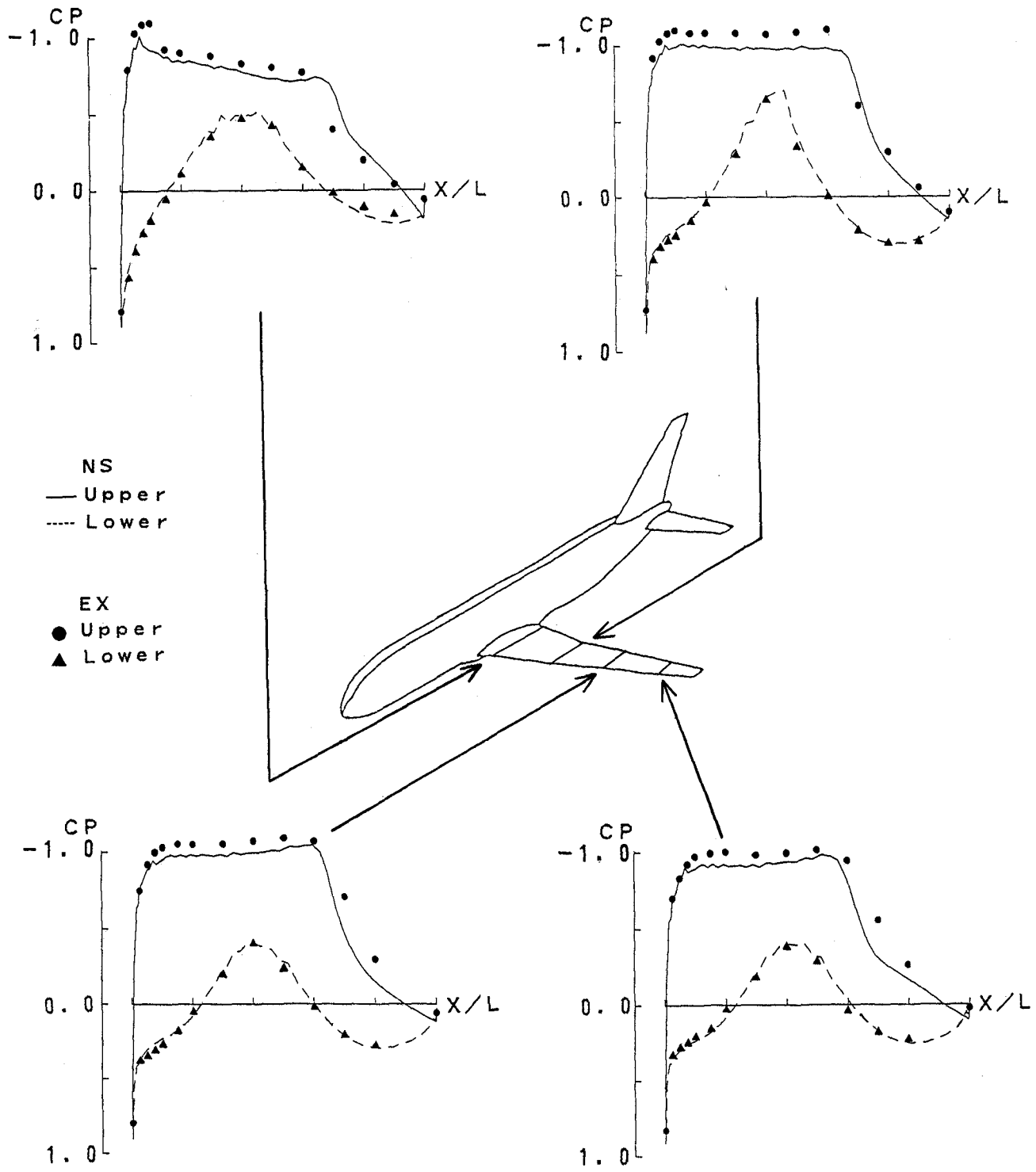

(b) Wing Surfaces at Four Different Spawise Stations

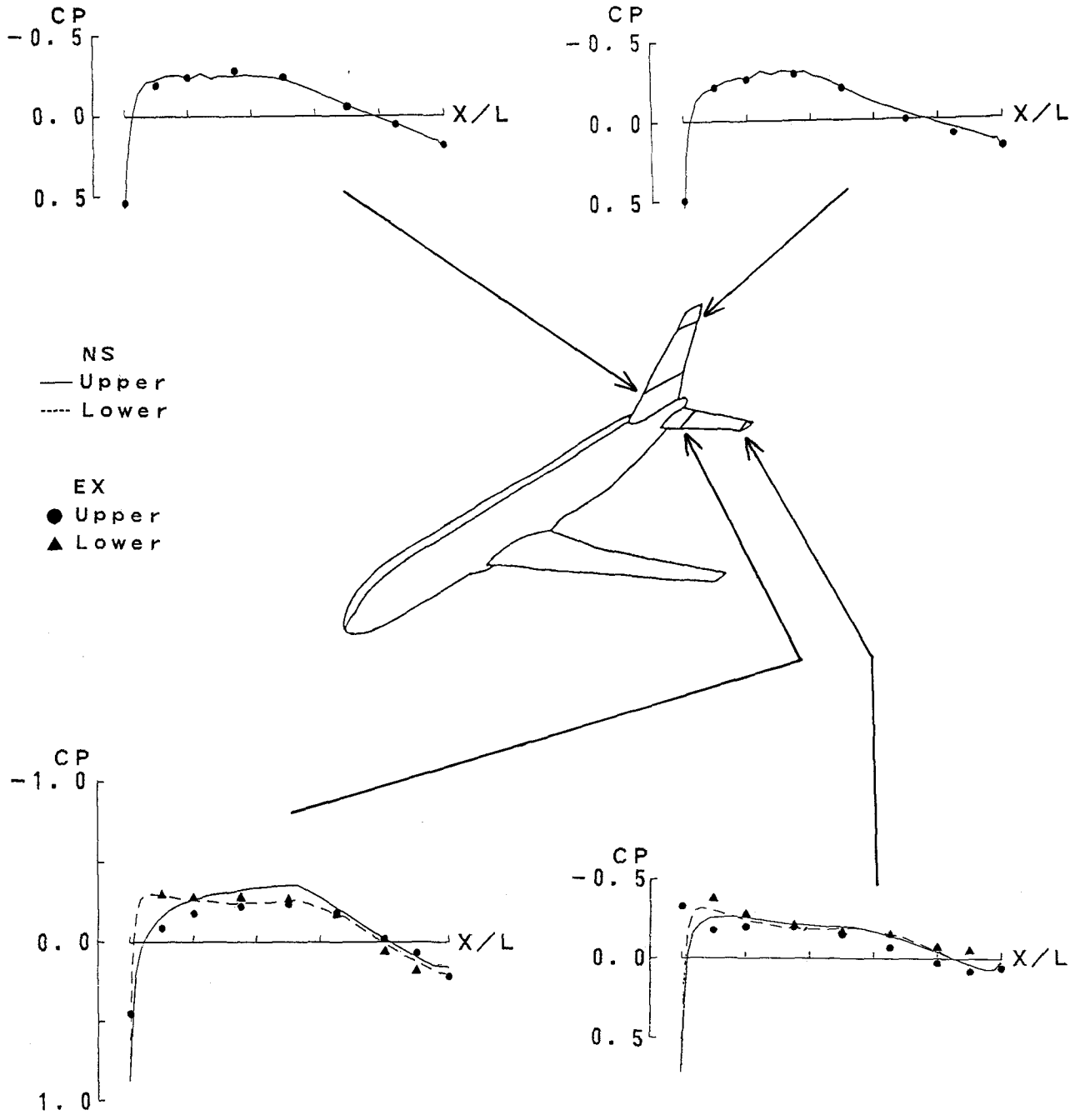

(c) Horizontal and Vertical Tails

Fig.8 Comparison of Computed Pressure Distributions with Experimental Data for Transonic Aircraft Configuration

$M = 0.82$ $\alpha = 2°$ $R_e = 1.1 \times 10^6$